IOWA STATE UNIVERSITY
Digital Repository

Chemistry Publications

Chemistry

8-2013

Protein-Mimetic, Molecularly Imprinted Nanoparticles for Selective Binding of Bile Salt Derivatives in Water

Joseph K. Awino
Iowa State University

Yan Zhao
Iowa State University, zhaoy@iastate.edu

Follow this and additional works at: http://lib.dr.iastate.edu/chem_pubs

Part of the Chemistry Commons

The complete bibliographic information for this item can be found at http://lib.dr.iastate.edu/chem_pubs/187. For information on how to cite this item, please visit http://lib.dr.iastate.edu/howtocite.html.

Protein-Mimetic, Molecularly Imprinted Nanoparticles for Selective Binding of Bile Salt Derivatives in Water

Abstract

A tripropargylammonium surfactant with a methacrylate-terminated hydrophobic tail was combined with a bile salt derivative, divinyl benzene (DVB), and a photo-cross-linker above its critical micelle concentration (CMC). Surface-cross-linking with a diazide, surface-functionalization with an azido sugar derivative, and free-radical-core-cross-linking under UV irradiation yielded molecularly imprinted nanoparticles (MINPs) with template-specific binding pockets. The MINPs resemble protein receptors in size, complete water-solubility, and tailored binding sites in their hydrophobic cores. Strong and selective binding of bile salt derivatives was obtained, depending on the cross-linking density of the system.

Disciplines
Chemistry

Protein-Mimetic, Molecularly Imprinted Nanoparticles for Selective Binding of Bile Salt Derivatives in Water

Joseph K. Awino and Yan Zhao*

Department of Chemistry, Iowa State University, Ames, Iowa 50011-3111, United States

S *Supporting Information*

ABSTRACT: A tripropargylammonium surfactant with a methacrylate-terminated hydrophobic tail was combined with a bile salt derivative, divinyl benzene (DVB), and a photo-cross-linker above its critical micelle concentration (CMC). Surface-cross-linking with a diazide, surface-functionalization with an azido sugar derivative, and free-radical-core-cross-linking under UV irradiation yielded molecularly imprinted nanoparticles (MINPs) with template-specific binding pockets. The MINPs resemble protein receptors in size, complete water-solubility, and tailored binding sites in their hydrophobic cores. Strong and selective binding of bile salt derivatives was obtained, depending on the cross-linking density of the system.

Molecularly imprinted polymers (MIPs) have binding sites potentially complementary to guests in size, shape, and distribution of functional groups.[1−3] They are usually prepared by copolymerization of functional monomers and cross-linkers in the presence of a template. Tremendous progress has been made in the last decades in this technology, with imprinted materials generated for small and large guests,[1−3] in macroporous polymers and on surface[4] for molecular recognition and catalysis,[5,6] and even unimolecularly within dendrimers.[7,8]
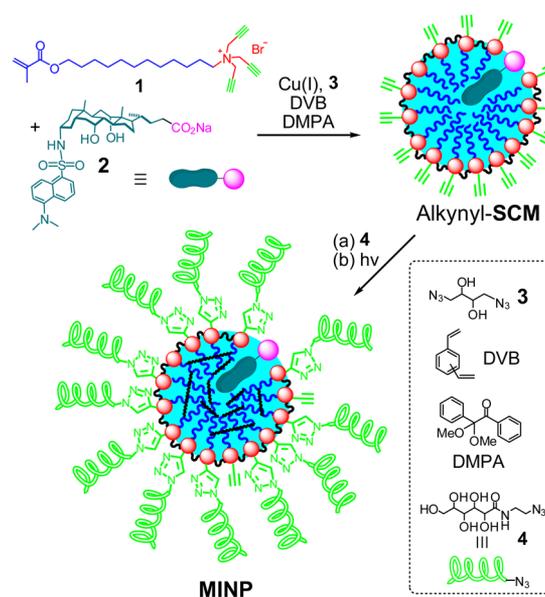
A difficult challenge in molecular imprinting remains the creation of protein-like, water-soluble nanoparticles with high binding affinity and selectivity for guests.[9−11] Part of the challenge comes from the general difficulty in constructing synthetic receptors that function in water.[12] Hydrogen bonds as directional intermolecular forces are the most popular tools used by chemists for molecular recognition but tend to become ineffective in aqueous solution due to competition from the solvent. The hydrophobicity of typical MIPs represents another hurdle, as hydrophobic materials often bind nonpolar molecules nonspecifically.

In this communication, we report a method to prepare molecularly imprinted nanoparticles (MINPs) for selective binding of bile salt derivatives in water. Although imprinted polymeric nanoparticles have been reported in the literature,[13−15] our MINP is characterized by its discrete binding sites and great resemblance to protein receptors in its nanodimension, complete water-solubility, functionalizable exterior, and easily accessible, tailor-made hydrophobic binding pocket. We chose bile salts as the template/guest molecules because of their important biological properties and water-solubility.[16,17]

The key design in our MINPs is the doubly cross-linkable surfactant **1**. The tripropargylated surfactant forms micelles in water with a high density of alkyne on the surface. Covalent fixation by a diazide cross-linker using Cu(I) catalysts yields surface-cross-linked micelles (SCMs) that could be easily functionalized through another round of click reaction.[18−21] Unlike previously synthesized tripropargylated surfactants, however, **1** has a polymerizable methacrylate and thus can undergo free-radical polymerization *orthogonal* to the surface-cross-linking by the click reaction.

Surfactant **1** has three alkyne groups, and cross-linker **3** has two azides. In the first stage of the reaction, we performed the surface-cross-linking of the micelles using [**3**]:[**1**] = 1.2/1, allowing good cross-linking while leaving sufficient alkyne groups on the SCM surface for further functionalization (Scheme 1).[18−21] The cross-linked micelles were prepared with 10 mM of **1** in water, above its CMC of 0.55 mM (Figure 1S in Supporting Information). Our DLS study showed that each SCM contained ca. 50 surfactants (Figure 2S). Thus, a ratio of [**1**]:[**2**] = 1:0.02 in theory placed one template (i.e., bile salt derivative **2**) within each SCM. The cross-linking chemistry and covalent structure of

Scheme 1. Preparation of MINP

ACS Publications   © 2013 American Chemical Society

12552

dx.doi.org/10.1021/ja406089c | *J. Am. Chem. Soc.* 2013, 135, 12552−12555

the SCMs have been previously characterized by mass spectrometry and TEM.[18]

After surface-cross-linking, sugar-derived ligand **4** was added to the reaction mixture. The surface functionalization, catalyzed also by Cu(I), made the final MINPs completely hydrophilic and easy to purify (vide infra). After surface functionalization, the sample was immediately subjected to UV irradiation to copolymerize the methacrylate of **1** and DVB solubilized within the SCMs. The photopolymerization was initiated by DMPA (i.e., 2,2-dimethoxy-2-phenylacetophenone, a photoinitiator) added together with DVB at the beginning of the reaction. After 12 h of irradiation, ^{1}H NMR spectroscopy indicated complete disappearance of alkenic protons (Figure 3S). DLS showed a narrow distribution of nanoparticles ca. 4.2 nm in diameter for alkynyl-SCM, 5.9 nm after surface functionalization, and 5.0 nm after core-cross-linking (Figure 4S).

Preparation of the MINPs was remarkably simple. The entire synthesis was a one-pot reaction over 2 d at room temperature in water. Equally important was the extremely easy purification. The nanoparticles could be precipitated from acetone after the core-cross-linking, due to the sugar-derived surface ligand **4**. Repeated washing by methanol/acetic acid and methanol completely removed the template (as shown by fluorescence spectroscopy) and afforded the final MINPs in ca. 80% yield. The materials obtained were fully soluble in water and showed no change in size compared to the as synthesized MINPs.

An important strategy in the MINP synthesis was the combination of a cationic cross-linkable surfactant and an anionic template. Their electrostatic interactions make it easy to not only incorporate the template inside the micelle and ultimately inside MINP, but also orient the hydrophobic part of template within the hydrophobic core of the micelle and the carboxylate on the surface. The result is easy removal of the template, which vacates the binding site, and facile rebinding of the guest.

The dansyl group of **2** allowed us to study its binding by fluorescence spectroscopy. As shown in Figure 1a, upon the
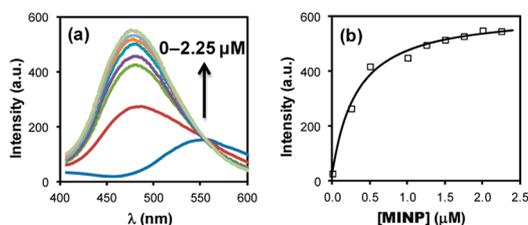
Figure 1. (a) Emission spectra of **2** upon the addition of different concentrations of MINP(**2**). [**2**] = 0.050 μM. The concentration of MINP was calculated based on a MW of 49800 g/mol determined by DLS (see Figure 5S for details). (b) Nonlinear least-squares fitting of the emission intensity of **3** at 475 nm to a 1:1 binding isotherm.

addition of MINP(**2**), i.e., MINP imprinted against **2**, to an aqueous solution of **2**, the dansyl emission at 550 nm immediately shifted to 475 nm. A large blue shift and enhanced emission suggest a more hydrophobic environment around dansyl[22] and are frequently observed when dansyl-labeled compounds are internalized by micelles.[23,24] The fluorescence intensity at 475 nm fitted nicely to a 1:1 binding isotherm to give an association constant (K_a) of 3.3×10^6 M^{-1} (Figure 1b). The binding affinity was among the highest observed between synthetic hosts and steroid derivatives including bile salt derivatives.[17]

After confirming effective binding of the template molecule, we studied the binding of several other bile salt derivatives (**5**–**9**) to understand the selectivity of the MINPs. After all, molecular imprinting is meant to create binding sites complementary to the template. Among these compounds, **5** and **6** have the acyl group on the amine gradually decrease in size and were designed to test the size/shape selectivity of the MINPs.
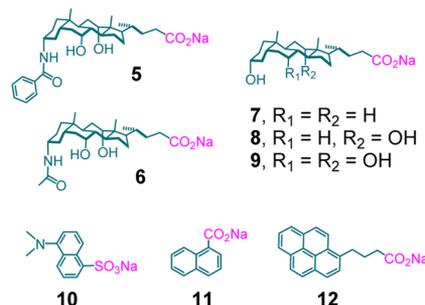

Table 1 summarizes the binding data of MINPs generated from **2** and **6** as the templates. For the majority of the bindings, we employed isothermal titration calorimetry (ITC) because most of the guests were not fluorescent. An important benefit of ITC is the simultaneous determination of the number of binding sites (N) on the MINP. Figure 2 shows three typical ITC titration curves between MINP(**2**) and bile salt derivatives. Note that, for the fluorescent guest (**2**), the binding constants obtained by the fluorescence titration and ITC showed excellent agreement (Table 1, compare entries 1 & 2 and 10 & 11).

Our first batch of MINPs was prepared with 0.5 equiv of DVB. ITC shows that MINP(**2**) synthesized under this condition bound its template with $K_a = 3.5 \times 10^6$ M^{-1} (Table 1, entry 2). As the acyl group decreased in size, the binding deteriorated, with K_a going down to 2.5×10^6 for the benzoyl derivative (**5**) and to 0.05×10^6 when the benzoyl was replaced by acetyl. In other words, the template itself fitted the binding pocket better than the other two (smaller) analogues, demonstrating the effectiveness of the imprinting. Among the naturally occurring bile salts, **7** showed similar binding as **6** but none of the more hydrophilic compounds (**8** and **9**) gave any detectable binding.

We then synthesized MINPs using the smaller bile salt derivative **6** as the template. The result was somewhat disappointing. On the one hand, the largest bile salt (**2**) showed weaker binding to MINP(**6**) than to MINP(**2**), as expected from the smaller size of the binding pocket in the former (Table 1, compare entries 2 and 6). On the other hand, although **2** bound to MINP(**6**) less strongly than **5**, both compounds bound much more strongly than **6** itself ($K_a = 0.09 \times 10^6$ M^{-1}). It appears that both hydrophobic effects and size/shape selectivity were playing roles in this MINP. Essentially, although the binding pocket of MINP(**6**) was smaller than that of MINP(**2**), the stronger hydrophobicity of **2** and **5** gave them a larger driving force to occupy the hydrophobic pocket than the somewhat hydrophilic **6**. Whereas **6** might fit the binding site of MINP(**6**) better than the larger bile salts, its weaker hydrophobicity lowers its tendency to enter the pocket.

Not satisfied with the above results, we decided to increase the amount of DVB to 1 equiv to **1** for the core-cross-linking. This was the highest amount of DVB that could be solubilized by the surfactant in water. To our delight, binding selectivity increased dramatically. Using this more highly cross-linked MINP(**2**), we were able to distinguish the size of the acyl group easily: the dansyl, benzoyl, and acetyl derivatives afforded K_a of 3.5, 0.46,

Table 1. Binding Data for MINPs (Obtained by ITC unless Indicated Otherwise)[a]

entry	MINP	DVB (equiv)	guest	K_a ($\times 10^6$ M^{-1})	$-\Delta G$ (kcal/mol)	N
1	MINP(2)	0.5	2	3.3 ± 0.5[b]	8.9	-[b]
2	MINP(2)	0.5	2	3.5 ± 0.2	8.9	1.0
3	MINP(2)	0.5	5	2.5 ± 0.1	8.7	0.9
4	MINP(2)	0.5	6	0.05 ± 0.01	6.4	0.7
5	MINP(2)	0.5	7	0.03 ± 0.01	6.0	0.3[c]
6	MINP(6)	0.5	2	1.39 ± 0.02	8.4	0.5
7	MINP(6)	0.5	5	1.99 ± 0.03	8.6	0.7
8	MINP(6)	0.5	6	0.09 ± 0.01	6.8	0.8
9	MINP(6)	0.5	7	0.02 ± 0.01	5.9	0.2[c]
10	MINP(2)	1.0	2	3.7 ± 0.8[b]	9.0	-[b]
11	MINP(2)	1.0	2	3.5 ± 0.2	8.9	1.0
12	MINP(2)	1.0	5	0.46 ± 0.07	7.7	0.7
13	MINP(2)	1.0	6	0.28 ± 0.04	7.4	0.6
14	MINP(2)	1.0	7	-[d]	-[d]	-[d]
15	MINP(2)	1.0	10	0.07 ± 0.01	6.6	0.3[c]
16	MINP(2)	1.0	11	0.0045 ± 0.0002	5.0	0.2[c]
17	MINP(2)	1.0	12	0.28 ± 0.03	7.4	0.6
18	MINP(2)	1.0	2[e]	3.21 ± 0.02	8.9	1.0
19	MINP(2)	1.0	2[f]	3.28 ± 0.02	8.9	1.0
20	MINP(6)	1.0	2	0.27 ± 0.12	7.4	0.7
21	MINP(6)	1.0	5	0.58 ± 0.02	7.9	0.6
22	MINP(6)	1.0	6	1.1 ± 0.2	8.2	0.8
23	MINP(6)	1.0	7	-[d]	-[d]	-[d]
24	MINP(2)$_2$[g]	1.0	2	3.56 ± 0.01	8.9	1.2
				3.07 ± 0.04	8.8	1.2

[a]The titrations were generally performed in duplicates and the errors between the runs were <10%. Binding was measured in 50 mM Tris buffer (pH = 7.4) with 150 mM NaCl unless otherwise noted. Compounds **8** and **9** showed no detectable binding by ITC with any of the MINPs. [b]Binding data were obtained from fluorescence titration using a 1:1 binding model. [c]The weak binding made the curve fitting not as accurate. [d]Binding (K_a <1000 M^{-1}) was not detectable by ITC. [e]Binding was measured in 50 mM Tris buffer (pH = 7.4) with 200 mM NaCl. [f]Binding was measured in 50 mM Tris buffer (pH = 7.4) without NaCl. [g]The MINPs were prepared with [**1**]:[**2**] = 1:0.04, i.e., twice as much of the template was employed as compared to other examples. The two binding constants were for the two independent binding sites, respectively.
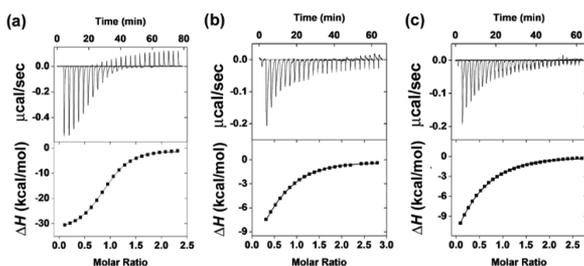
Figure 2. ITC titration curves obtained at 298 K for the binding of **2** (a), **5** (b), and **6** (c) by MINP(2) prepared with 1 equiv of DVB. The data correspond to entries 11–13 in Table 1. Additional ITC titration curves can be found in the Supporting Information (Figures 6S–10S). In general, an aqueous solution of an appropriate bile salt in Tris buffer (50 mM Tris, 150 mM NaCl, pH = 7.4) was injected in equal steps into 1.428 mL of the corresponding MINP solution (4.0 mg/mL) in the same buffer. The top panel shows the raw calorimetric data. The area under each peak represents the amount of heat generated at each ejection and is plotted against the molar ratio of the bile salt to the MINP. The smooth solid line is the best fit of the experimental data to the sequential binding of N equal and independent binding sites on the MINP. The heat of dilution for the bile salt, obtained by adding the bile salt to the buffer, was subtracted from the heat released during the binding. Binding parameters were autogenerated after curve fitting using Microcal Origin 7.

and 0.28×10^6 M^{-1}, respectively (Table 1, entries 11–13). Lithocholate **7** displayed no binding at all.

For the more highly cross-linked MINP(2), we also studied several non-steroid aromatic guests (**10**–**12**) to test the binding selectivity. Dansyl sulfonate **10** in a sense was a "half-match" for the binding site generated from dansylated **2**. Its K_a ($= 0.07 \times 10^6$ M^{-1}) was reduced by ca. 50 times from that of **2**. A further decrease of the hydrophobic size made naphthalene-1-carboxylate (**11**) an even poorer guest, whose K_a was only 0.0045×10^6 M^{-1} or about 800 times weaker than that of **2**. As soon as the guest size increased, binding resumed, as pyrenebutyrate **12** displayed identical binding constant to that of **6** ($K_a = 0.28 \times 10^6$ M^{-1}) or 1/13 of that of **2**.

All the bindings were measured in 50 mM Tris buffer with 150 mM NaCl. When the salt concentration was raised to 300 mM, the MINPs were found to precipitate out of the buffer. In 200 and 0 mM NaCl (Table 1, entries 18 and 19), similar binding constants were obtained for the MINP(2)–**2** complex and were essentially within the experimental error from that in 150 mM NaCl (entry 11). We attributed the insensitivity of binding to salt (at least over 0–200 mM NaCl) to the two opposing binding forces present in the system: whereas salt tends to strengthen hydrophobic interactions, it weakens the electrostatic interactions between the positively charged MINP and the negatively charged guest.

Importantly, when 1 equiv of DVB was used in the core-cross-linking, selective binding pockets could be created for the smaller bile salt **6** as well. As the acyl group became smaller, the bile salts exhibited a consistent *increase* in their binding affinity toward the

highly cross-linked MINP(**6**), with K_a increasing from 0.27×10^6 to 0.58×10^6 and further to $1.1 \times 10^6 \, M^{-1}$ (entries 20−22). This trend was opposite to the hydrophobicity of the guest and different from what was observed for MINP(**6**) prepared with 0.5 equiv of DVB. Clearly, the higher cross-linking density of the material significantly enhanced the rigidity of the binding pockets. Under this condition, even though the more hydrophobic guests (**2** and **5**) possess stronger thermodynamic "desires" to enter the hydrophobic pocket, they were excluded most likely because of their misfit to the less "forgiving" binding sites.

It should be pointed out that, unlike conventional MIPS and the reported molecularly imprinted nanoparticles,[13−15] our MINPs on average possessed approximately one guest-binding site per particle. Except when weak binding made the curve fitting less accurate, the number of independent binding sites (N) obtained by ITC was close to 1 in most cases for the MINPs (Table 1). This feature comes directly from the stoichiometry of template used in the synthesis relative to the micelle aggregation number of **1**.

To demonstrate the tunability in binding stoichiometry, we prepared MINP(**2**)$_2$ with [**1**]:[**2**] = 1:0.04, i.e., doubling the amount of template employed during the imprinting. Figure 3
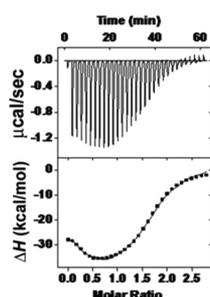
Figure 3. ITC titration curves obtained at 298 K for the binding of **2** by MINP(**2**)$_2$ prepared with 1 equiv of DVB. The data correspond to entry 24 in Table 1. The smooth solid line is the best fit of the experimental data to the sequential binding of 2 equal and independent binding sites on the MINP.

shows the ITC titration curve for the rebinding of **2**. The distinctively different curve as compared to those in Figure 2 fitted best to a binding model with two independent binding sites per nanoparticle. As shown by entry 24 in Table 1, the two binding sites had very similar binding constants ($K_a = 3.56$ and $3.07 \times 10^6 \, M^{-1}$), which were essentially the same as that of the MINP(**2**)−**2** complex ($K_a = 3.5 \times 10^6 \, M^{-1}$). Thus, the same hydrophobic and electrostatic interactions were behind all these binding events, whether the MINP contained one or two binding sites.

To summarize, we have developed a facile method to create protein-like, water-soluble receptors for selective binding of bile salt derivatives in water. Unlike proteins, however, these nanoparticles are extremely robust and have outstanding tolerance for organic solvents and adverse temperature/pH conditions. The robustness comes directly from their highly cross-linked nature and was demonstrated by our washing conditions in the purification. Their nanodimension, readily modified structure,[18−21,25−27] and excellent properties of molecular recognition should make them highly useful materials for chemistry and biology.

ASSOCIATED CONTENT

Ⓢ Supporting Information

Experimental details for the syntheses, DLS data, ITC titration curves, and NMR spectra for key compounds. This material is available free of charge via the Internet at http://pubs.acs.org.

AUTHOR INFORMATION

Corresponding Author

zhaoy@iastate.edu

Notes

The authors declare no competing financial interest.

ACKNOWLEDGMENTS

REFERENCES

(1) Wulff, G. *Angew. Chem., Int. Ed. Engl.* **1995**, *34*, 1812.

(2) Mosbach, K.; Ramström, O. *Nat. Biotechnol.* **1996**, *14*, 163.

(3) Haupt, K.; Mosbach, K. *Chem. Rev.* **2000**, *100*, 2495.

(4) Sellergren, B. *Molecularly Imprinted Polymers: Man-Made Mimics of Antibodies and Their Applications in Analytical Chemistry*; Elsevier: Amsterdam, 2001.

(5) Wulff, G. *Chem. Rev.* **2001**, *102*, 1.

(6) Komiyama, M. *Molecular Imprinting: From Fundamentals to Applications*; Wiley-VCH: Weinheim, 2003.

(7) Zimmerman, S. C.; Wendland, M. S.; Rakow, N. A.; Zharov, I.; Suslick, K. S. *Nature* **2002**, *418*, 399.

(8) Zimmerman, S. C.; Zharov, I.; Wendland, M. S.; Rakow, N. A.; Suslick, K. S. *J. Am. Chem. Soc.* **2003**, *125*, 13504.

(9) Dirion, B.; Cobb, Z.; Schillinger, E.; Andersson, L. I.; Sellergren, B. *J. Am. Chem. Soc.* **2003**, *125*, 15101.

(10) Cutivet, A.; Schembri, C.; Kovensky, J.; Haupt, K. *J. Am. Chem. Soc.* **2009**, *131*, 14699.

(11) Ma, Y.; Pan, G. Q.; Zhang, Y.; Guo, X. Z.; Zhang, H. Q. *Angew. Chem., Int. Ed.* **2013**, *52*, 1511.

(12) Oshovsky, G. V.; Reinhoudt, D. N.; Verboom, W. *Angew. Chem., Int. Ed.* **2007**, *46*, 2366.

(13) Hoshino, Y.; Kodama, T.; Okahata, Y.; Shea, K. J. *J. Am. Chem. Soc.* **2008**, *130*, 15242.

(14) Yang, K. G.; Berg, M. M.; Zhao, C. S.; Ye, L. *Macromolecules* **2009**, *42*, 8739.

(15) Zeng, Z. Y.; Patel, J.; Lee, S. H.; McCallum, M.; Tyagi, A.; Yan, M. D.; Shea, K. J. *J. Am. Chem. Soc.* **2012**, *134*, 2681.

(16) Danielsson, H.; Sjövall, J. *Sterols and Bile Acids*; Elsevier: Amsterdam, 1985.

(17) Wallimann, P.; Marti, T.; Furer, A.; Diederich, F. *Chem. Rev.* **1997**, *97*, 1567.

(18) Zhang, S.; Zhao, Y. *Macromolecules* **2010**, *43*, 4020.

(19) Zhang, S.; Zhao, Y. *J. Am. Chem. Soc.* **2010**, *132*, 10642.

(20) Li, X.; Zhao, Y. *Bioconjugate Chem.* **2012**, *23*, 1721.

(21) Peng, H.-Q.; Chen, Y.-Z.; Zhao, Y.; Yang, Q.-Z.; Wu, L.-Z.; Tung, C.-H.; Zhang, L.-P.; Tong, Q.-X. *Angew. Chem., Int. Ed.* **2012**, *51*, 2088.

(22) Li, Y. H.; Chan, L. M.; Tyer, L.; Moody, R. T.; Himel, C. M.; Hercules, D. M. *J. Am. Chem. Soc.* **1975**, *97*, 3118.

(23) Zhong, Z.; Zhao, Y. *J. Org. Chem.* **2008**, *73*, 5498.

(24) Zhao, Y. *J. Org. Chem.* **2009**, *74*, 834.

(25) Li, X.; Zhao, Y. *Langmuir* **2012**, *28*, 4152.

(26) Zhang, S.; Zhao, Y. *Chem. Commun.* **2012**, *48*, 9998.

(27) Chadha, G.; Zhao, Y. *J. Colloid Interface Sci.* **2013**, *390*, 151.